

## Accepted Manuscript

Strengthening of slab-column connection against punching shear failure with CFRP laminates

Hikmatullah Akhundzada, Ted Donchev, Diana Petkova

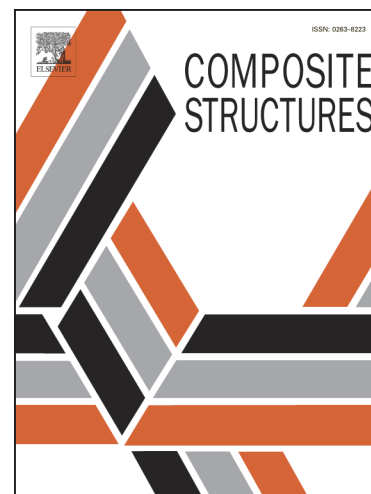
PII: S0263-8223(18)31454-5  
DOI: <https://doi.org/10.1016/j.compstruct.2018.09.076>  
Reference: COST 10223

To appear in: *Composite Structures*

Received Date: 19 April 2018  
Revised Date: 20 August 2018  
Accepted Date: 21 September 2018

Please cite this article as: Akhundzada, H., Donchev, T., Petkova, D., Strengthening of slab-column connection against punching shear failure with CFRP laminates, *Composite Structures* (2018), doi: <https://doi.org/10.1016/j.compstruct.2018.09.076>

This is a PDF file of an unedited manuscript that has been accepted for publication. As a service to our customers we are providing this early version of the manuscript. The manuscript will undergo copyediting, typesetting, and review of the resulting proof before it is published in its final form. Please note that during the production process errors may be discovered which could affect the content, and all legal disclaimers that apply to the journal pertain.



# Strengthening of slab-column connection against punching shear failure with CFRP laminates

Hikmatullah Akhundzada<sup>a,\*</sup> Ted Donchev<sup>a</sup> Diana Petkova<sup>a</sup>

<sup>a</sup> Department of Civil Engineering, Kingston University, London, UK

## Abstract

This paper presents the findings of an experimental investigation undertaken to evaluate the influence of externally bonded CFRP laminates on the punching shear capacity of a two-way spanning slab-column connection. Two control and five strengthened RC slabs were prepared and tested under concentrated load. The variables of the experiment were the anchorage type and width of the CFRP plates used. The structural response of the samples in terms of load, deflection, strain and cracking was monitored and analysed throughout the experimental procedure. It was found that strengthening increases the ultimate load by up to 25% and reduces the maximum deflection by up to 50%. The strengthening increases the cracking load and significantly reduces the cumulative length of radial cracks. The samples strengthened with transverse anchorages exhibited significantly high level of residual strength. The experimental findings for unstrengthened cases are compared with several design codes.

**Keywords:** reinforced concrete, flat slab, slab-column, punching shear, CFRP & strengthening.

## 1. Introduction & Background

RC flat slabs have been extensively used as structural systems over many years due to many attractive inherent qualities. The absence of dropped beams results in increased storey height, simple formwork and prompt construction. The slab-column connection is susceptible to failure due to high level of shear stresses resulting in punching shear which can potentially lead to progressive collapse.

Strengthening of existing RC flat slabs is often required to restore or to increase the initial designed capacity especially in multi-storey car parks and office buildings. The capacity of flat slabs could be increased by strengthening it directly with shear reinforcement or indirectly with flexural reinforcement. A direct correlation between the amount of flexural reinforcement and increase in punching shear capacity has been reported [1, 2, 3].

FRP materials have been studied over the past two decades in the field of structural engineering and it fulfils the shortcomings associated with the use of steel plate retrofitting. The further optimisation of FRP for strengthening flat slabs would be beneficial for providing a sustainable solution to the problem.

Research has been conducted on the effectiveness of strengthening flat slabs with CFRP sheets/laminates against punching shear failure.

Harajli and Soudki [4] retrofitted flat slabs with CFRP sheets on the tension surface and reported that it improves the flexural and shear capacity by 17 - 45%. They suspected that the rise in load due to increased flexural capacity would change the failure mode from flexural to shear. The increase in capacity was directly proportional to the area of CFRP.



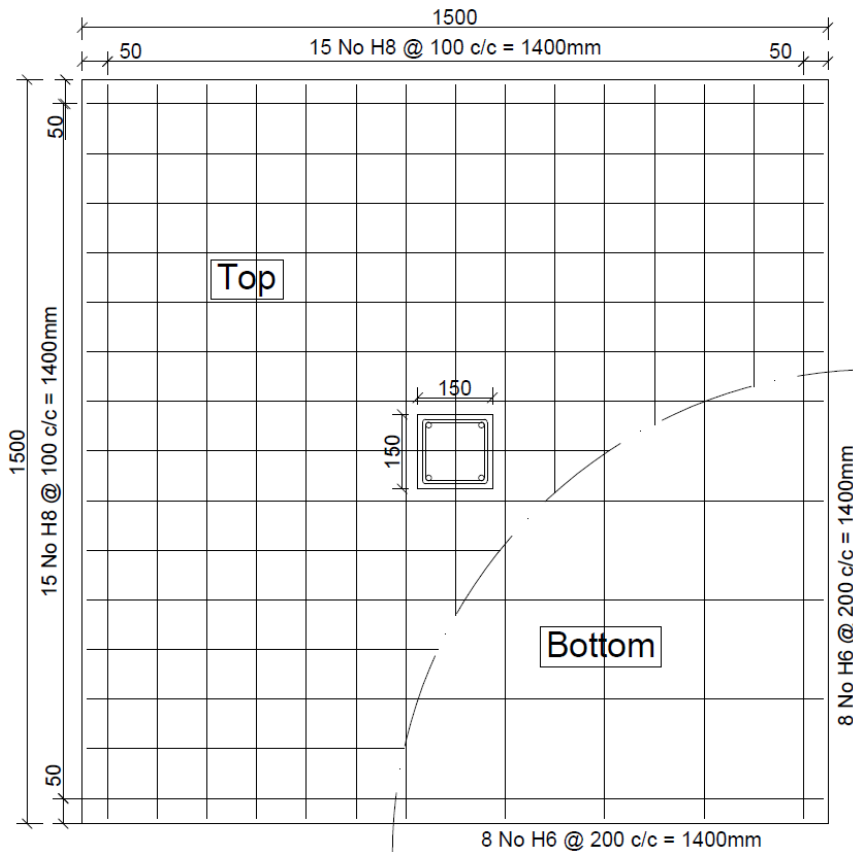


**Fig. 2.** Plan view, reinforcement details and geometry

## 2.2 Material properties

The concrete was provided by an external supplier to emulate real world building construction and was mixed on site. The concrete pour was executed in two separate days from two batches, resulting into grouping the samples into two series. Slump tests were conducted before casting to determine the workability and consistency of the concrete mix. Liquid water based curing compound was applied to the surface of the slab after 3 hours of casting to prevent moisture evaporation from the mix. All the samples were covered with wet hessian sheets for the duration of the curing. A combination of concrete cubes 150x150x150mm and cylinders 150x300mm were tested to obtain the uniaxial compressive strength of concrete. The compressive strength of concrete determined on the day of testing ranged between 30 to 35.5 MPa.

The EP Structural Adhesive used in this study is made of two part comprising Bisphenol A/F epoxy resin with a modified aliphatic polyamine hardener and inert filler [10]. The EP structural adhesive has a mixing ratio of 1:2.4 of hardener to resin material. The adhesive reaches compressive strength of 70 N/mm<sup>2</sup> within 24 hours of mixing. The CFRP laminates were manufactured by S&P, Switzerland, with fibre volumetric content up to 70% in an epoxy resin matrix. The unidirectional laminates used were S&P CFK 200/2000. The properties of CFRP plates used in the study are shown in table 1 [11].

**Table 1:** Properties of CFRP

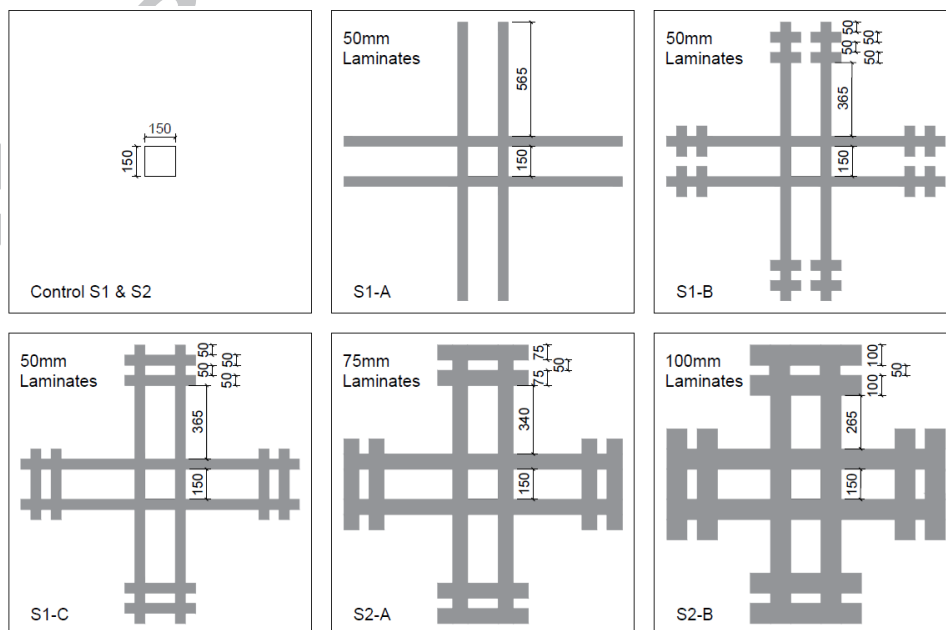
Fibre	Fibre content (%)	Density (g/cm <sup>3</sup> )	Thickness (mm)	Elastic modulus (kN/mm <sup>2</sup> )	Tensile strength (N/mm <sup>2</sup> )
Carbon	70	1.7	1.2	>210	2400-2600

### 2.3 Strengthening Scheme

The samples are divided into two series as they are casted from two different concrete batches. There are two un-strengthened control samples and one sample for each strengthening type. Series one consists of one control sample and three samples strengthened with 50 mm wide CFRP plates positioned around the perimeter of the column. The influence of the non-bolted anchorage system is investigated in series one. The anchorage type used for sample S1-B in series one is based on Donchev's and Nabi's [12] findings for beams. The anchorage type is modified, developed and is applied for the remaining samples. Series two includes one control and two strengthened samples with 75 mm and 100 mm wide CFRP plates. The effect of the width of CFRP plates is investigated in series two as shown in table 2 & Fig 3.

**Table 2.** Description of the samples

Series	Specimen	CFRP Width (mm)	Anchorage Type	Compressive Strength (MPa)
I	S1-Control	N/A	N/A	31
	S1-A	50	N/A	31.5
	S1-B	50	2 no. 50x150	30
	S1-C	50	50x350	35.5
II	S2-Control	N/A	N/A	32
	S2-A	75	75x450	30.5
	S2-B	100	100x550	30

**Fig. 3.** Strengthening scheme

## 2.4 Specimen preparation

The CFRP plates were bonded to the tension surface of the slab 7 days before the testing. A wire brush attached to an angle grinder was used to get uniform exposure of the aggregates. The surface of the concrete was cleaned by vacuum cleaner and white spirit to ensure dust free surface. The adhesive was then applied in thin layers on both the surface of CFRP and concrete in order to avoid development of entrapped air within the adhesive while attaching the two surfaces. The CFRP laminates were then pressed until a uniform layer of epoxy with thickness of 2-3mm was achieved. The residue epoxy squeezed from the sides was cleared with a scrapper to create a finished angle of  $45^\circ$  between the CFRP and substrate. The epoxy was left to cure at  $20^\circ\text{C}$  in the lab.

FRP anchorage systems are primarily used to delay or prevent the debonding process because of low tensile strength of concrete [13]. One of the key purposes of anchorage system is to provide stress transfer mechanism where no bond sufficient length is available beyond the critical section [14]. FRP anchorage system is chosen for this research due to size restriction of the samples to achieve the required bonded length. This anchorage type could be modelled in real structure as having longer longitudinal CFRP plates which would serve as fixed anchors. Although, the bolted anchorage system are highly efficient compared to the FRP anchorage system but it is more intrusive to RC structures [14].

## 2.5 Instrumentation & test set-up

The experimental setup is shown in Fig. 4, 5 & 6. Six strain gauges were attached to the tension surface of the concrete two of them at centre and four at quarter span of the slab. Further four strain gauges were positioned at mid-point of the CFRP laminates. The LVDTs were placed at centre and quarter-span of the slab to capture the deflection. Four dial gauges were positioned at mid-point of each of the sides of the supporting frame to monitor movement of the frame as shown in Fig 4 and 6. A light steel frame was built above the testing rig to support the instrumentation independently.

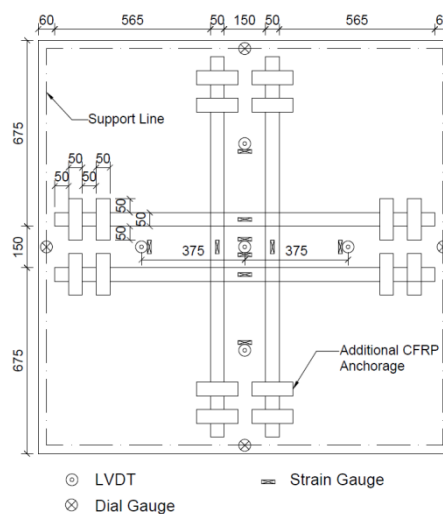


**Fig. 4.** Instrumentation set-up

The slab was supported on L shaped angles on all four sides and the load was applied through a hydraulic jack positioned under the column head. Smooth surface rebar were placed between the L shaped angles at the top and the slab to allow for free rotation of the slab at the support. The spacing of the angles above and below the slab is 200mm which allowed for free rotation of the slab at the edges. The slabs did not interact directly with the supporting angle profiles during the test. The load cell was placed over the hydraulic jack and the load was distributed to the column head using a stress distributing steel plate. The direction of applying the load was upwards in reverse to a real life structure. The frame was bolted to a strong concrete floor. The sensors and the load cell were connected to a data logger which captured the data at rate of 10 readings/sec. The load was gradually applied at rate of 1 kN/min.

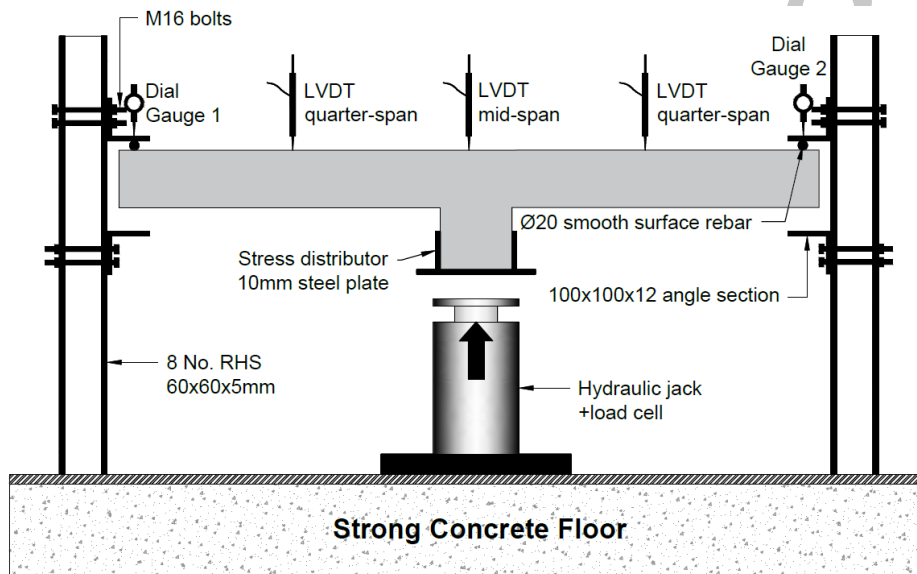


**Fig. 5.** Side view of test set-up



**Fig. 6.** Test set-up

### 3. Results and discussion

#### 3.1 Failure characteristics

The recorded load was corrected to account for the variation of the strength of concrete which varied from 30 to 35.5 MPa amongst the seven specimens tested. The load values were multiplied by  $\sqrt{31.5/f_c}$  to account for minor shifts in uniaxial compressive strength of concrete which affects the punching shear capacity. The average compressive strength of the two control samples is 31.5MPa.

The control samples in series one and two failed under classical punching shear failure. The failure was abrupt and sudden which was followed by sudden drop in the load at failure point. The first crack appeared at the tension surface of the slab close to the perimeter of the column at the load of 58 kN for sample S1-Control. While the first crack for sample S2-Control appeared at load of 55 kN roughly at the centre of the slab. Concrete is not a homogenous materials and such differences are within the expected limits.

Sample S1-A suffered from premature debonding of the CFRP from surface of the concrete. The first crack appeared at load of 60 kN running from one end through the centreline of the slab to the other end. The first crack intersected two of the laminates at the centre point. The initial debonding was localised close to the quarter span of the slab. The full debonding of one of the strips of CFRP from mid-span to the end of laminates occurred as the load increased. A sudden drop in the stiffness of the sample was observed as the full debonding happened. The sample failed suddenly in a punching shear failure mode.

The performance of the samples with additional CFRP anchorages S1-B, S1-C, S2-A and S2-B was very similar. The initial debonding appeared close to the quarter-length of the longitudinal laminates between the additional anchorages and the central intersection point for these samples. Continuous development of radial cracks resulted in localised debonding of the individual strips of the laminates. However, the longitudinal strips were fixed by additional anchorages at the ends. It resulted in relatively stiffer response from the samples towards the later stages of the loading. It was evident that by increasing the width of the CFRP plates the appearance of the first crack was delayed. The final failure mode was classical punching shear for all the samples. The addition of transverse anchorages contributed towards enhancing the capacity of strengthened samples. Partial debonding of the strips was observed at earlier stages (around load level 150 – 160 kN) for the strengthened samples. The debonding of the anchorages appeared at later stages of loading which was followed by punching shear.

#### 3.2 Load versus deflection

The load deflection graph for test series one is shown in Fig 7. The strengthened samples in series one had very similar behaviour as the control sample throughout the initial stages of loading. The load vs deflection relationship was almost linear and the samples had relatively high stiffness up to load level of 60 kN attributed to uncracked concrete section. A significant increase in the rate of deflection could be observed after formation of extensive cracking.

Sample S1-Control displayed the lowest level of stiffness throughout the loading and failed abruptly after reaching to the maximum load. Sample S1-A did not have additional transverse CFRP anchorages but exhibited somewhat stiffer response than the control

sample. A sudden drop of the load at 160 kN could be observed, which shows the debonding of more than 50% of CFRP from the surface of the concrete. The stiffness of the sample reduced significantly after debonding of the laminates and started behaving in a similar way as the control sample.

Sample S1-B displayed higher stiffness and displayed higher ultimate load in comparison to S1-Control and S1-A. Partial bond failure of the strips was observed at its quarter length after reaching load levels of 150 kN. The sudden drop at load of 195 kN shows failure of the first transverse anchorage but the remainder of the anchorages continued to act and retained significant level of loading. The sample failed under punching shear after failure of the anchorages at load of 200 kN.

The highest ultimate capacity in series one was shown by sample S1-C which reached peak load of 219 kN. The higher capacity and flexural stiffness of this sample could be associated with the anchorage type (see Fig 3). The partial bond failure of the longitudinal strips started after reaching load level of 150 - 160 kN and kept increasing with the load. The rapid drop at load of 211 kN, 219 kN and 183 kN shows debonding of the transverse anchorages.

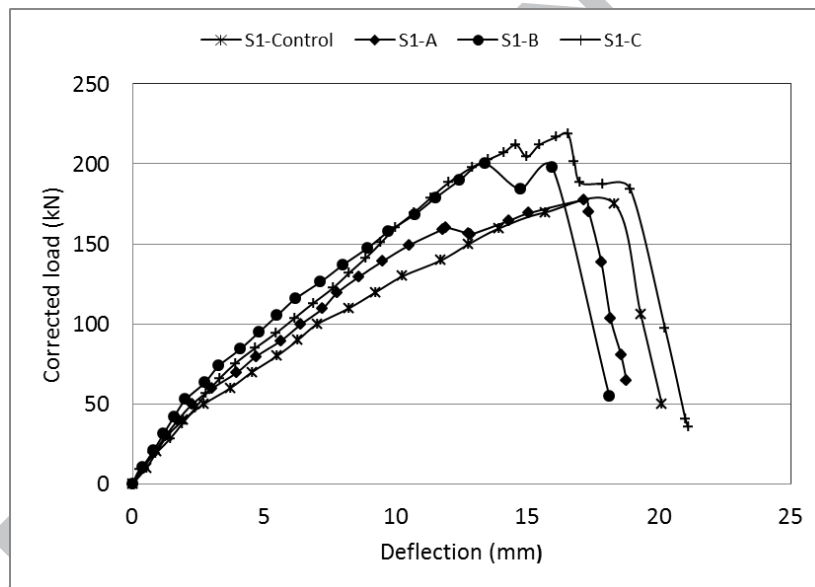


**Fig. 7.** Load vs deflection above the column head for series 1

The load deflection graph for series two is shown in Fig 8. The load deflection relationship for the control sample in series two was very similar to the graph of control sample in series one. Sample S2-A and S2-B displayed the highest level of stiffness throughout the loading. It could be associated with the larger area of laminates providing increase of the load at the same level of deformation. The failure of these samples started with debonding of one of the transverse anchorages but the full failure did not occur until debonding of the most of the anchorages.

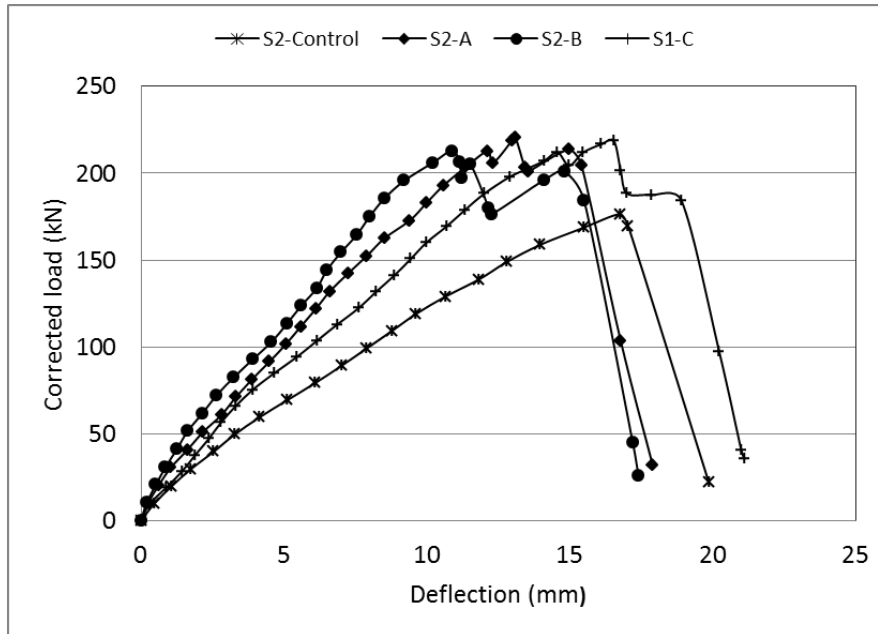


**Fig. 8.** Load vs deflection above the column head for series 2

The key observation for failure of the samples with transverse anchorages was their ability to sustain residual load for considerable level of deformation after reaching the first peak load. This indicates more gradual and ductile mode of destruction. The additional CFRP laminates in transverse direction hold the longitudinal plates at each end and act as fixed anchors. The performance of anchorage type for sample S1-C was significantly superior to anchorage type for sample S1-B in terms of ultimate capacity, debonding and flexural stiffness.

It should be noted that the deflection of each of the samples was considerably higher after the development of extensive cracking. All of the samples went through higher level of cracking between loads of 80 – 120 kN. Fig 9 shows the deflection of the control sample for series one at different stages of loading.

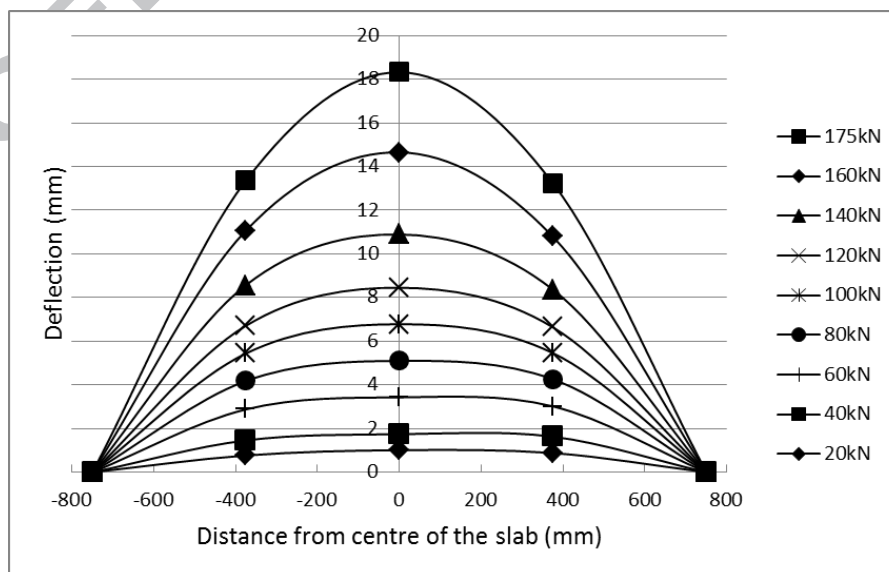


**Fig. 9.** 3 point deflection of sample (S1-control)

### 3.3 CFRP strain

The load vs strain relationship for the longitudinal CFRP reinforcement at their centre-line is shown in Fig 10. All samples exhibited significantly lower level of strain at the initial stages of loading which could be associated to development of micro-cracking within the slab. The development of radial and shear cracks for level of loadings between 30 kN & 50 kN resulted in a higher level of strain with increasing load.

The highest level of strain at any given point during the loading was displayed by sample S1-A which could be related to lack of additional transverse anchorages. Development of cracking under the laminates caused localised debonding between loads of 145 kN to 165 kN. The laminates had premature debonding at loading of 160 kN which resulted in significant reduction of the strain.

Localised debonding of the plates could be observed for sample S1-B roughly at the same level of loading to sample S1-A. The primary cause of this behaviour is development of cracks which causes localised failure of the bond. However, the sample S1-B exhibited significantly higher level of loading which is achieved by the anchorages positioned at each end of longitudinal laminates. The maximum level of strain was exhibited for sample S1-C which reached peak value of around 4000 microstrain. The debonding of the transverse anchorages could be confirmed at the load of 211 kN, 219 kN and 183 kN by observing sudden drops in the load.

Sample S2-A went through localized debonding at load of 170 kN to 180 kN which is confirmed by rapid drop of strain. The sample with 100mm wide laminates S2-B reached strains level of 2200 microstrain as maximum value which is considerably lower in comparison with other samples. The sudden decline of the strain shows full debonding of the longitudinal laminates which was followed by failure of the sample.

It is evident that the larger area of CFRP plates results in lower level of strain and vice versa. This could be fundamentally caused by distribution of force over a given area which results in varying degree of strain within the tested samples. The rupture strength for the CFRP is around 16000 microstrains, and none of the sample reached to 25% of the maximum limit. It confirms that the ultimate capacity of the material is not utilized thus pointing to the aim to prevent brittle failure due to rupture of laminates. However, the increase of width of laminate above 50mm seems ineffective of increasing the load capacity of the strengthened samples. From another point of view, reducing the width of laminates could result in earlier debonding of the longitudinal due to insufficient area between adhesive and concrete to transfer shear stresses.

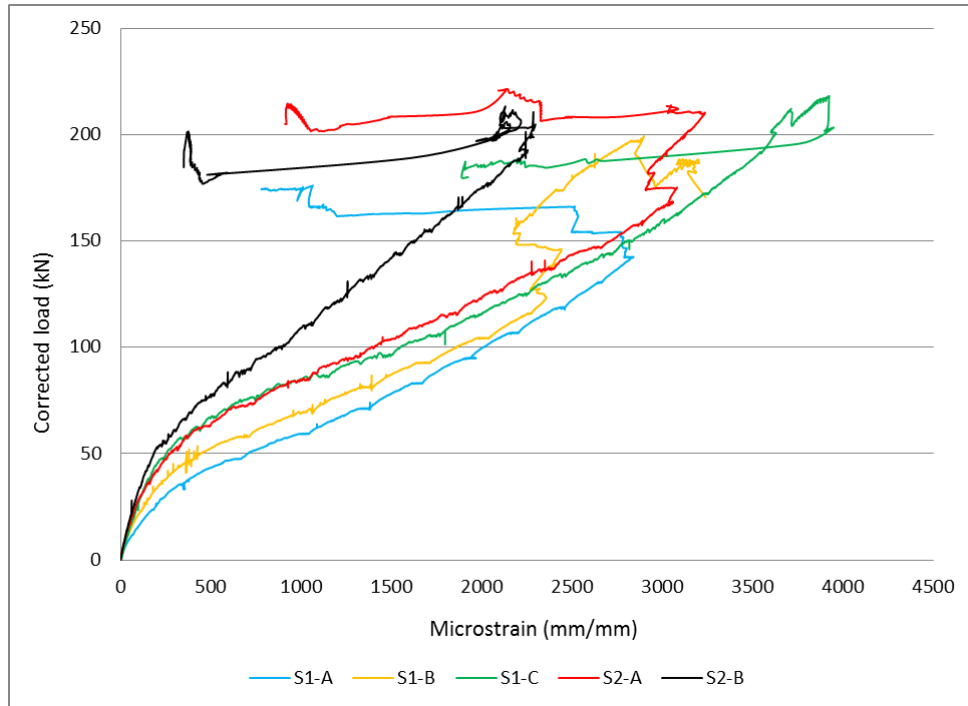


**Fig. 10.** Load vs strain in CFRP laminates

### 3.4 Crack propagation

It was evident that the addition of CFRP plates resulted in increasing the cracking load. A direct correlation between the surface area of the CFRP and the load at appearance of the first crack could be observed in table 3. The first crack appeared at the load of 58 kN and 55 kN for both the control samples in series one and two. The cracking load, for the samples with 50 mm wide laminates exhibited slight improvement in comparison with control samples. The highest improvement in cracking load was shown by sample S2-B strengthened with 100 mm wide laminates. In most cases, the radial cracks started developing from the centre of the slabs and propagated towards the corners and edges.

A significant reduction in the number and the cumulative length of the radial cracks could be observed with increase of the surface area of CFRP. The sample strengthened with 100 mm wide laminates exhibited only 33% of the radial cracks observed in the control sample. Meanwhile, the crack propagation and the total length of radial cracks were very similar for all samples with 50 mm wide laminates. On average a reduction 50% in total length of radial cracks was recorded for samples with 50 mm wide laminates in comparison to control samples. It should be noted that cracks crossing under the laminates are not included.

The punching shear crack for the control samples in series one and two developed towards the later stages of the loading and the shape was roughly circular as shown in Fig 11. However, the punching shear crack for samples S1-B, S1-C and S2-A moved towards the transverse anchorages. The shapes of those cracks were roughly elliptical and L-shaped. The plan area of the punching shear crack does not have direct connection with the ultimate capacity. Probably the ultimate capacity is influenced by debonding of the anchoring zone of the plates. The failure mode of the tested samples is shown in Fig 12.

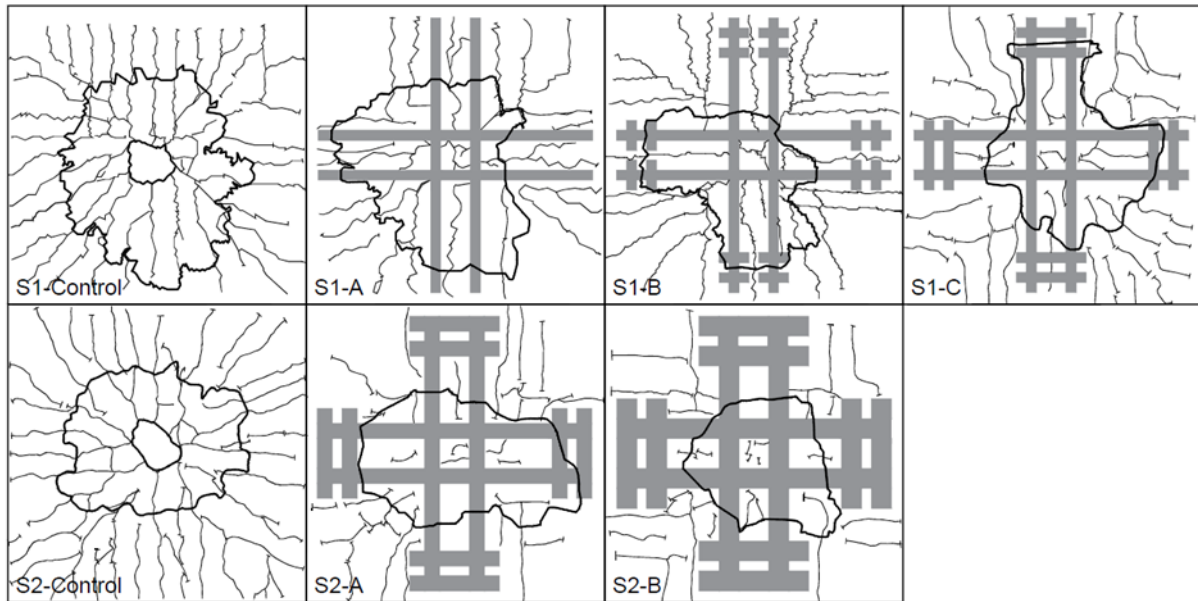


**Fig. 11.** Radial and punching shear cracks

A direct correlation between cracking and the central deflection of the samples could be observed i.e. the deflection was higher for severely cracked samples and vice versa. The observed rate of crack development was relatively high during the application of the load from 80 to 130 kN. The cracking load and the total length of the crack for each sample is shown in table 3.

**Table 3:** Cracking load & total length of radial cracks

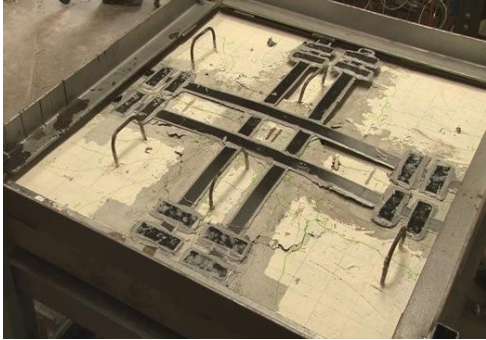
	S1-Control	S1-A	S1-B	S1-C	S2-control	S2-A	S2-B
Cracking Load (kN)	58	60	62	66	55	70	73
Total length of radial cracks (m)	20.1	13.7	13.5	14.2	21.2	8.9	8.3



S1-Control



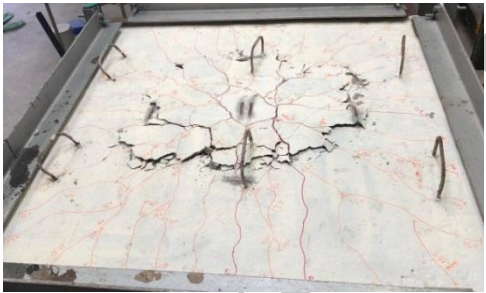
S1-A



S1-B



S1-C



S2-Control



S2-A



S2-B

**Fig. 12.** Failure mode of all samples

### 3.5 Ultimate capacity

The ultimate capacities of the tested samples are presented in Fig 13. It was found that application of longitudinal CFRP plates without additional anchorages experiences premature debonding and do not contribute towards improving the maximum load. Addition of CFRP anchorages to an identical strengthening layout increases the peak load by 13% and 25% for samples S1-B and S1-C respectively compared to control sample. It appears that the anchorage layout used for sample S1-C is considerably more effective. This anchorage system enables the transfer of stresses between the two main parallel CFRP plates which results in delayed failure of the plates.

The performance of the strengthened samples in terms of ultimate load in series two was very similar to each other. Samples S2-A, S2-B and S1-C reached to maximum load of 221 kN, 213 kN and 219 kN respectively, before failing under punching shear. The average increase in ultimate capacity for series two is over 24% in comparison to the control sample. It suggests that increasing the width of the CFRP plates above 50mm for this specific scale of slab reduced cracking and deflections, but did not increase the ultimate load. The reason for the early debonding for samples S2-A and S2-B could be development of cracking under the laminates which would initiate the debonding process.

The strengthened samples with transverse anchorages maintained to carry more than 90% of their ultimate load before the point of failure (refer to Fig 7 & 8). This shows a rather ductile behaviour which could be used as warning signs for the failure. This behaviour is described as residual load which is obtained by dividing the ultimate load by last peak value of load from Fig 7 & 8.

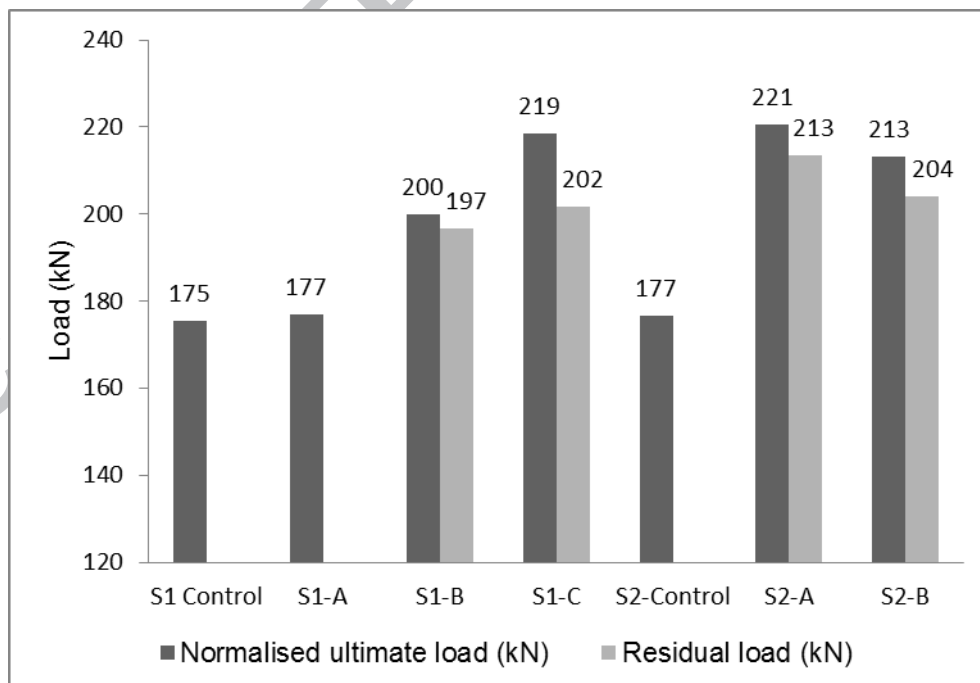


**Fig. 13.** Ultimate and residual load

#### 4. Punching shear in design codes

Existing design codes and guidance documents provide numerical approach to calculate the punching shear capacity of flat slabs without shear reinforcement. The unstrengthened control cases can be compared against Eurocode 2 [15], ACI Code 318-14 [16] and FIB Model Code 2010 [17]. The punching shear design principle is based on the identification of a critical section (control perimeter) in slab-column connection and checking the shear capacity at those locations. It should be noted that the safety factors for material properties and actions have been ignored in the expressions presented herein.

##### 4.1 Eurocode 2

The design principle for flat slabs without shear reinforcement for Eurocode 2 [15] is adopted on the basis of FIB Model Code 1990 with only minor modifications [18]. Eurocode 2 demands that the shear resistance is checked along different control parameters for flat slabs without shear reinforcement. The shear stresses along the first control parameter, located at the periphery of the loaded area  $u_0$ , must be lower than the web-crushing limit for beams. Also, the shear stresses must be lower than the punching shear resistance at the second control parameter  $u_1$  which is located at distance of  $2.0d$  from the periphery of the loaded area. A load increase factor  $\beta$  is considered to take into account the load eccentricities and non-uniform shear stress distribution around the perimeter of the column. The load increase factor  $\beta$  for non-sway structures where the lengths of adjacent spans do not differ by more than 25% could be taken as 1.15 for interior columns. The punching shear resistance of the critical section of flat slabs according to Eurocode 2 is shown in expression below:

$$V_c = C_{Rd,c} k (100 \rho_1 \cdot f_{ck})^{1/3} + k_1 \sigma_{cp} \geq (V_{min} + k_1 \sigma_{cp}) \quad (1)$$

$$C_{Rd,c} = \frac{0.18}{\gamma_c} \quad (2)$$

$$k = 1 + \sqrt{200/d} \leq 2 \quad (3)$$

$$\rho = \sqrt{(\rho_{1z} \cdot \rho_{1y})} \leq 0.02 \quad (4)$$

$$V_{min} = 0.035 k^{3/2} f_{ck}^{1/2} \quad (5)$$

In the expression above  $\gamma_c$  is the partial safety factor for concrete which is taken as 1.0 for experimental purposes. The term  $k$  is a size factor for effective depth; the term  $\rho_1$  is the average reinforcement ratio and the term  $f_{ck}$  is the characteristic compressive strength of concrete based on cylindrical strength. The term  $k_1$  is an empirical factor with recommended value of 0.1 which shows normal stresses. The concrete stresses in critical section is denoted by  $\sigma_{cp}$  which could normally be attributed to prestressing. The expression  $V_{min}$  represents the minimum shear capacity.

#### 4.2 FIB Model Code 2010

The FIB Model Code 2010 [17] provides a new design theory for predicting the punching shear strength of flat slabs. The design concept is developed on the basis of critical shear crack theory which is established from the width of shear crack [19], [20], [21]. The width of shear crack is dependent on rotation of the slab which takes several factors into account. The FIB Model Code 2010 reduces the length of critical parameter to  $0.5d$  to take into account the load eccentricity and non-uniform shear stress distribution. The shear capacity of flat slab is given in expression 6.

$$V_{rc} = k_{\psi} \frac{f_{ck}}{\gamma_c} \times b_0 \times d_v \quad (6)$$

The parameter  $k_{\psi}$  takes into account the deformations (rotations) of the slabs and is derived from:

$$k_{\psi} = \frac{1}{1.5 + 0.9k_{dg}\psi d} \leq 0.6 \quad (7)$$

The parameter  $k_{dg}$  depends on the maximum aggregate size used in the concrete mix.  $d_g$ , used in the concrete mix.

$$k_{dg} = \frac{32}{16 + d_g} \quad (8)$$

The term  $\psi$  denotes the angle of rotation which could be obtained from expression 9. The FIB Model Code 2010 provides two levels of approximation for rotation of the slab. The level one approximation is used for slabs without considerable redistribution of forces whilst the level two approximation is used for slabs for significant redistribution of bending moment. The level one approximation is applied due to testing of isolated flat slabs.

$$\psi = 1.5 \times \frac{r_s f_{yd}}{d E_s} \quad (9)$$

Where  $r_s$  shows the radius of separated slab element;  $f_{yd}$  shows the yield strength of flexural steel reinforcement and  $E_s$  shows the elastic modulus of the flexural reinforcement.

#### 4.3 ACI building code 318-14

The ACI building code [16] requires checking the shear capacity of flat slabs at the periphery of the column and at critical perimeter which is located at  $0.5d$  from the column face. The shear capacity is related to the compressive strength of concrete and the contribution of flexural reinforcement is not taken into account. The punching shear resistance is given in expression 10.

$$V_c = 1/3 \cdot d \cdot u \sqrt{f_c'} \quad (10)$$

The term  $u$  shows the control (critical) perimeter of the slab-column connection.

#### 4.4 Comparison with experimental results

The experimental and predicted ultimate capacities for the samples are presented in table 5. Despite adopting different approaches, the prediction of failure load for Eurocode 2, ACI 318 and FIB Model Code 2010 is in great correspondence with each other. It should be noted that the values for ultimate load are only valid for the given boundary conditions. Their approaches accurately predict the failure load of the slabs. It is clear that the strength of concrete plays a significant role amongst the three codes in predicting the punching shear capacity. The data presented in Table 4 is used for calculating the theoretical capacity of the slabs.

Table 4: Parameter used in design codes

d (mm)	c (mm)	$f_c$ (MPa)	$r_s$ (mm)	$k_{dg}$ (mm)	$f_{yd}$ (MPa)	$E_s$ (GPa)
102	150	Variable	725	32	450	210

Table 5: Comparison of experimental results and code predictions

Samples	$V_{u, test}$ (kN)	$V_{u, predicted}$ (kN)			$V_{u, test} / V_{u, predicted}$		
		EC2	ACI	FIB	EC2	ACI	FIB
S1-Control	175	161	159	164	1.09	1.10	1.07
S2-Control	177	162	161	166	1.09	1.10	1.06

#### 5. Discussion

The non-anchored strengthened sample suffered from premature debonding due to insufficient bonded length of the CFRP strips. Anchoring the CFRP strips delays the debonding and results in higher ultimate capacity. The anchorage type used for sample S1-C, S2-A and S2-B delivers similar ultimate load which is higher compared to S1-B. This anchorage type allows for transfer of forces between the two parallel CFRP strips, enabling the strengthening to act as a system together, whereas, the CFRP strips in sample S1-B acts individually.

The experiment could be improved by testing a larger section of the slab, as it appears the punching shear crack seems to grow into the anchoring zone. Providing longer bonded length for the CFRP strips with the proposed anchorage system could potentially perform better in a real life structure. Development of numerical simulation for parametric studies and taking the size effect into consideration is needed for developing design formulas.

## 6. Conclusion

The strengthening of flat slabs against punching shear failure is experimentally investigated in this study and the main conclusions are summarized below:

1. The use of non-bolted anchorage system delays the debonding of CFRP plates and improves the structural response of the tested samples. The modified anchorage used for sample S1-C increased the ultimate load by 25% and was found to be the most effective layout considering the amount of CFRP used.
2. The samples with transverse anchorages exhibited relatively gradual mode of destruction with secondary increase of the load after initial debonding.
3. Increasing the width of CFRP laminates over 50mm for this specific scale of slab does not increase the ultimate load. The failure is initiated by debonding of the laminates thus not utilizing the maximum capacity of the CFRP laminates.
4. The flexural stiffness (load/vertical deflection) of strengthened samples was considerably higher in comparison to control samples. Sample S2-B exhibited the highest stiffness resulting in an increase of over 100% in comparison to the control samples.
5. The strengthening improves the cracking load and significantly reduces the total length of radial cracks. Sample S2-B displayed 40% fewer radial cracks in comparison to the control samples.
6. Eurocode 2, the FIB model code 2010 and the ACI 318 provides accurate predictions of the punching shear capacity of column supported slabs.

## References

- [1] Moe, J. (1961) Shearing strength of reinforced concrete slabs and footings under concentrated loads, development department bulletin No. D47, Portland Cement Association, Skokie 11. pp130.
- [2] Yitzhaki, D. Punching strength of reinforced concrete slabs. ACI. 1996. 63(5) p. 527 – 561.
- [3] Kinnunen, S. Nylander, H. Punching of concrete slabs without shear reinforcement, Transactions, No. 158. 1960, Royal Institute of Technology: Stockholm, Sweden.
- [4] Harajli, MH. Soudki, KA. Shear Strengthening of Interior Slab–Column Connections Using Carbon Fiber-Reinforced Polymer Sheets. Journal of Composites for Construction 2003; 7(145): 145 – 153.
- [5] Esfahani, MR. Kianoush, MR. Moradi, AR. Punching shear strength of interior slab–column connections strengthened with carbon fiber reinforced polymer sheets. Engineering Structures 2009; (31): 1535 – 1542.
- [6] Agbossou, A. Micheal, L. Lagache, M. Hamelin, P. Strengthening slabs using externally-bonded strip composites: Analysis of concrete covers on the strengthening. Composites: Part B 2008; (39): 1125 – 1135.

- [7] Soudki, K. El-Sayed, AK. Vanzwol, T. Strengthening of concrete slab-column connections using CFRP strips. *Journal of King Saud University - Engineering Sciences* 2008; (24): 25 – 33.
- [8] Kim, YJ. Longworth, JM. Wight, RG. Green, MF. Punching shear of two-way slabs retrofitted with prestressed or non-prestressed CFRP sheets. *Journal of Reinforced Plastics and Composites* 2010; 29(8): 1206 – 1223.
- [9] Abdullah, A. Bailey, CG. Wu ZJ. Tests investigating the punching shear of a column-slab connection strengthened with non-prestressed or prestressed FRP plates. *Construction and Building Materials* 2013; (48): 1134 – 1144.
- [10] Weber Saint-Gobian. Moisture-tolerant epoxy adhesive for structural bonding application 2017.  
[https://www.netweber.co.uk/uploads/tx\\_weberproductpage/02.020A\\_webertec\\_EP\\_structural\\_adhesive\\_01.pdf](https://www.netweber.co.uk/uploads/tx_weberproductpage/02.020A_webertec_EP_structural_adhesive_01.pdf)
- [11] Weber Saint-Gobian. High performance carbon fibre plate reinforcement for structural strengthening. 2016.  
[https://www.netweber.co.uk/uploads/tx\\_weberproductpage/10.010\\_webertec\\_force\\_carbon\\_plate.pdf](https://www.netweber.co.uk/uploads/tx_weberproductpage/10.010_webertec_force_carbon_plate.pdf)
- [12] Donchev. T, Nabi. P. (2010) Non-bolted anchorage systems for CFRP laminates applied for strengthening of RC slabs: The 5th International Conference on FRP Composites in Civil Engineering, September 27-29, Beijing, China.
- [13] Ceroni, F. Pecce, M. Matthys, S. Taerwe, L. Debonding strength and anchorage devices for reinforced concrete elements strengthened with FRP sheets. *Composites: Part B* 2008; (39) 429–441.
- [14] Grelle, SV. Sneed, LH. Review of Anchorage Systems for Externally Bonded FRP Laminates. *International Journal of Concrete Structures and Materials* 2013; 7(1): 17-33.
- [15] European Committee for Standardization: Eurocode 2. Design of concrete structures – part 1 – 1: General rules and rules for buildings 2004; pp. 225.
- [16] ACI Committee 318: Building code requirements for structural concrete and commentary (ACI 318-14), 2014; pp.525.
- [17] Federation internationale du beton. Fib model code for concrete structures. 2010; pp 230 – 231.
- [18] CEB-FIP Model Code 1990: Design Code, Thomas Telford, London, 1993.
- [19] Muttoni, A. Punching Shear Strength of Reinforced Concrete Slabs without Transverse Reinforcement. *ACI Structural Journal*, 105 (2008), pp. 440–450.
- [20] Ruiz, FM. Muttoni, A. Application of Critical Shear Crack Theory to Punching of Reinforced Concrete Slabs with Transverse Reinforcement. *ACI Structural Journal*, 106 (2009), pp. 485–494.
- [21] Muttoni, A., Ruiz, M. F.: The levels-of-approximation approach in MC 2010: application to punching shear provisions. *Structural Concrete*, 13 (2012), pp. 32–41, doi: 10.1002/suco.201100032.